Theoretical Calculations of Potential Energy Surface and Thermal Rate Constants for the H(Mu) + F_2 Reaction

Toshiyuki Takayanagi* and Yuzuru Kurosaki

Advanced Science Research Center, Japan Atomic Energy Research Institute, Tokai-mura, Naka-gun, Ibaraki 319-11, Japan

Received: April 24, 1997; In Final Form: July 14, 1997[⊗]

The potential energy surface of the H + F_2 → HF + F reaction has been calculated using the ab initio molecular orbital method at the CCSD/6-311++G(3DF,3PD) level of theory. We have found a collinear saddle point with a classical barrier height being 3.7 kcal/mol. Several important characteristics of the potential surface including the location of the saddle point, the bend angle dependence of the potential energy, and the long-range van der Waals interaction have been calculated. These data except for the barrier height were used to develop new potential energy surfaces. Thermal rate constants for the H + F_2 and Mu + F_2 reactions have been calculated with reduced dimensionality theory using new potential surfaces and compared to experimental results. It has been found that van der Waals interaction plays an important role in low-temperature behavior of rate constants, especially for Mu + F_2, where quantum mechanical tunneling should be dominant.

1. Introduction

The H + F_2 reaction is one of the prototypical atom−diatom chemical reactions and has also received considerable attention over the years because the reaction system is the basis of an efficient chemical laser. However, an accurate potential energy surface for this reaction has not yet been obtained due to the difficulty in performing highly accurate ab initio molecular orbital (MO) calculations. The first ab initio calculations were reported by Schaefer and co-workers.[1] They have done first-order configuration interaction (FOCI) calculations with a double-ζ basis set and obtained the barrier height of 1 kcal/mol although these calculations did not reproduce the experimental exothermicity of the reaction. The calculated classical barrier height can be compared with the experimental Arrhenius activation energy,[2,3] which has been reported to be 2.2−2.4 kcal/mol although the exact relationship between the Arrhenius activation energy and the classical barrier height is not so simple. Schaefer and co-workers[4] then improved their calculations by changing the double-ζ basis set into a polarized double-ζ one. The reaction exothermicity calculated with this basis set was considerably improved, but the barrier height was calculated to be 4.1 kcal/mol. Several years later, Dunning and co-workers[5] carried out the polarization configuration interaction (POL-CI) calculations with a polarized double-ζ basis set. The barrier height was calculated to be 5.2 kcal/mol, which is still larger than the experimental value, and the exothermicity calculated was in poor agreement with the experimental value.

Generally, it has been quite difficult to perform highly accurate ab initio calculations within chemical accuracy, which is sometimes considered to be 0.1 kcal/mol, because such a calculation requires large-scale CI as well as a larger basis set. The H + H_2 reaction has long been the only reaction whose potential energy surface has been obtained within chemical accuracy.[6] Also, it is quite recent that a highly accurate ab initio potential energy surface has been calculated for the F + H_2 reaction system.[7] Since both the H + H_2 and F + H_2 systems have fewer electrons than the H + F_2 system, it might be still difficult to obtain an accurate barrier height for the H + F_2 reaction. Nevertheless, ab initio MO calculations give important information other than the barrier height, such as location of the saddle point and a bend angle dependence of the potential at the saddle point. One of the purposes of the present work is to obtain such information from ab initio MO calculations in order to develop a new potential energy surface.

Several semiempirical potential energy surfaces have been proposed to date, including LEPS,[8−12] DIM,[13,14] and DIM-3C[15] functions. Among them, the extended LEPS potential empirically parametrized by Jonathan, Okuda, and Timlin[8] has been most extensively used in dynamics calculations, which we call the JOT surface hereafter. Previous dynamics calculations, including exact quantum collinear scattering calculations,[12,16−18] quasiclassical trajectory calculations,[9−11,19−22] distorted-wave Born approximation calculations,[23,24] and reactive infinite-order sudden calculations,[25] were carried out mostly to compare the vibrational distribution of the product HF on the JOT surface to experimental data.[8,26−30] Although the vibrational distributions calculated using various dynamical methods approximately reproduced the experimental results, thermal rate constants[31] calculated are not in good agreement with the experimental results,[32] especially for the Mu + F_2 reaction, where Mu (muonium) is a light "isotope" of hydrogen. The rate constants for Mu + F_2 calculated using variational transition state theory (VTST) with a sophisticated quantum mechanical tunneling correction are too large at high temperatures and too small at low temperatures.[32] These results qualitatively indicate that the Mu + F_2 kinetics provides a crucial test of the accuracy of the potential energy surface rather than the product vibrational distribution because the contribution of quantum tunneling is quite sensitive to the topography of the potential energy surface. In fact, Fleming and co-workers[32] stated that the theoretical rate constants calculated with the JOT potential energy surface underestimate the contribution of quantum mechanical tunneling.

In this paper we carry out extensive ab initio MO calculations to develop a new potential energy surface, with emphasis for obtaining better agreement of rate constants for H(Mu) + F_2 with experiment. The rate constants are calculated using reduced-dimensionality theory[33,34] developed by Bowman be-

* Corresponding author. E-mail address: tako@popsvr.tokai.jaeri.go.jp.
[⊗] Abstract published in *Advance ACS Abstracts,* September 1, 1997.

S1089-5639(97)01395-9 CCC: $14.00

TABLE 1: Saddle Point Properties for Various Potential Energy Surfaces

method	R(H−F) Å	R(F−F) Å	ΔE_b,[a] kcal/mol	ΔH kcal/mol	ω_{str}, cm^{-1}	ω_{bend}, cm^{-1}
ab initio						
FOCI/DZ[b]	2.05	1.57	1.0	88.3		
FOCI/DZP[c]	1.68	1.50	4.1	99.0		
POL-CI/DZP[d]	1.69	1.51	5.2	87.0		
CCSD/6-311++G(3DF,3PD)[e]	1.73	1.44	3.7	111.1	824	268
semiempirical						
JOT (LEPS)[f]	1.90	1.44	2.4	103.5	787	58
surface I (LEPS)[e]	1.75	1.44	0.7	103.5	792	204
surface II (LEPS)[e]	1.74	1.44	1.0	103.5	778	212
experiment			2.4 ± 0.2[g]	103.0[c]		
			2.2 ± 0.1[h]			

[a] All the theoretical values mean the classical barrier height without zero-point energy correction. [b] Reference 1. [c] Reference 3. [d] Reference 5. [e] Present work. [f] Reference 31. [g] Reference 2. [h] Reference 3.

TABLE 2: Total Energies (in au), Barrier Heights in (ΔE_b kcal/Mol), and Exothermicities (ΔH in kcal/mol) for the H + F_2 Reaction

method[a]	[HFF][b]	F	F_2[c]	HF[c]	ΔE_b[d]	ΔH
CCSD	−199.764 92	−99.613 62	−199.270 97	−100.334 29	3.7	111.1
CCSD(T)	−199.785 35	−99.617 59	−199.289 68	−100.341 39	2.6	106.4
QCISD	−199.766 06	−99.613 88	−199.272 16	−100.334 90	3.7	111.0
QCISD(T)	−199.786 07	−99.617 80	−199.290 18	−100.341 66	2.5	106.4

[a] All the methods employed the 6-311++G(3DF,3PD) basis set. The total energy of H atom for this basis set is −0.499 82 au. [b] The energies were calculated at the CCSD saddle point (R_{HF} = 1.73 and R_{FF} = 1.44 Å). [c] The energies were calculated at the geometry optimized by the same level of theory. [d] The classical barrier height without zero-point energy correction.

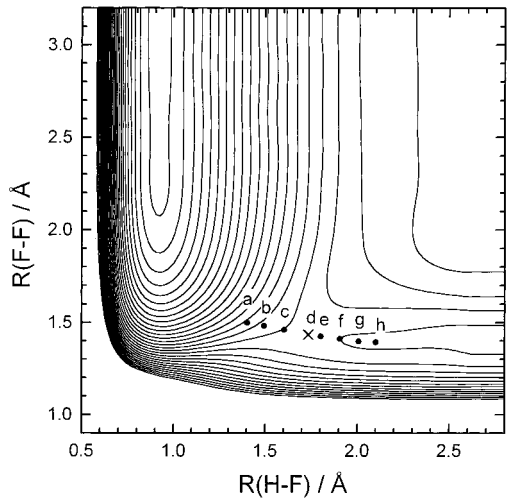

Figure 1. Contour plot of the linear HF_2 potential energy surface calculated at the CCSD/6-311++G(3DF,3PD) level of theory. The contour increment is 6.9 kcal/mol. The cross in the figure indicates the saddle point. The closed circles shown are the points where the bending potential were calculated (see Figure 2).

cause the theory is easier to do (enabling several iterations between surface development and dynamics calculations while the surface was being developed) and is reliable for calculating an accurate rate constant.

2. Ab Initio MO Calculations

Figure 1 shows a contour plot of the collinear HF_2 potential energy surface calculated at the CCSD level of theory with the 6-311++G(3DF,3PD) basis set. All the calculations were carried out using the Gaussian 94 package program.[35] About 200 points were calculated to draw this contour map. We can see that the saddle point occurs "early"; R(H−F) = 1.73 Å and R(F−F) = 1.44 Å. The barrier height was calculated to be 3.7 kcal/mol. Table 1 summarizes the location of the saddle point, the barrier height, the reaction exothermicity, and the vibrational frequencies and compares them with the earlier ab initio results as well as the semiempirical JOT result. Our saddle point geometry is found to be in good agreement with the FOCI/DZP result of Shaefer and co-workers[4] and with the POL-CI result of Dunning and co-workers.[5] Table 1 also reveals that the JOT surface has earlier saddle point than the present ab initio surface. The reaction exothermicity obtained at the CCSD level of theory, however, is found to be still in poor agreement with the experimental value; the calculated value is about 8 kcal/mol larger than the experimental one.

To study the effect of a higher order electron correlation on the barrier height and reaction exothermicity, we calculated them at other levels of theory including CCSD(T), QCISD, and QCISD(T), and the results are summarized in Table 2. The barrier heights were calculated using the saddle point geometry obtained from the CCSD calculations, but the geometries of HF and F_2 were optimized at each level of theory. Table 2 shows that CCSD and QCISD give almost similar results. We also find that inclusion of triple excitation reduces the barrier height and improves the reaction exothermicity significantly. However, we find that it is still difficult to obtain the barrier height and the exothermicity within chemical accuracy. The QCISD(T) level of theory gives the smallest barrier height, 2.5 kcal/mol, among the methods employed. Although this barrier height is quite close to the experimental activation energy shown in Table 1, we must conclude that the calculated barrier height should still include errors as large as a few kcal/mol because of disagreement in the reaction exothermicity.

Figure 2 shows the bend angle dependence of potential energy calculated at several points on the collinear minimum-energy path. The CCSD level of theory is found to predict the minimum-energy path to be collinear from Figure 2. This result is also consistent with the earlier FOCI ab initio calculation by Schaefer and co-workers.[1] The bending frequency at the saddle point can be calculated using the bending potential curve, and the result is included in Table 1. The most quantitative difference between the ab initio and the semiempirical JOT surface is that the JOT bending frequency is much smaller than the ab initio value; the present calculations predict that the ab initio transition state has a tighter structure than the semiempirical one. This result also leads to a simple prediction that the saddle point barrier height obtained from the ab initio

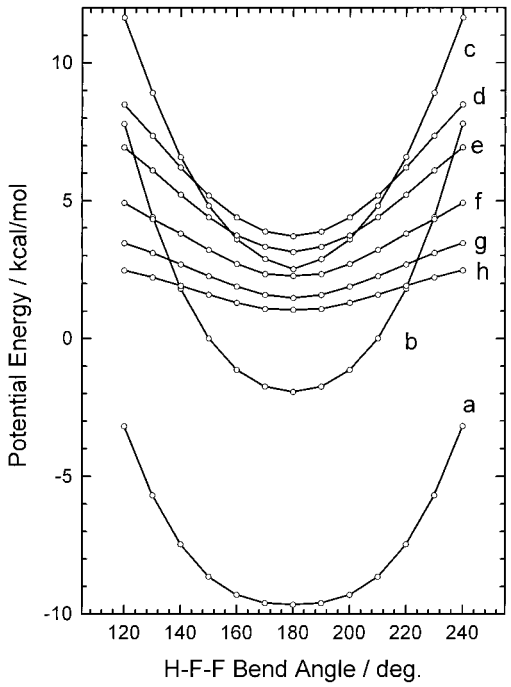

Figure 2. H−F−F bend angle dependence of potential energy at several points along the collinear minimum-energy path. (a)−(g) correspond to the points shown in Figure 1.

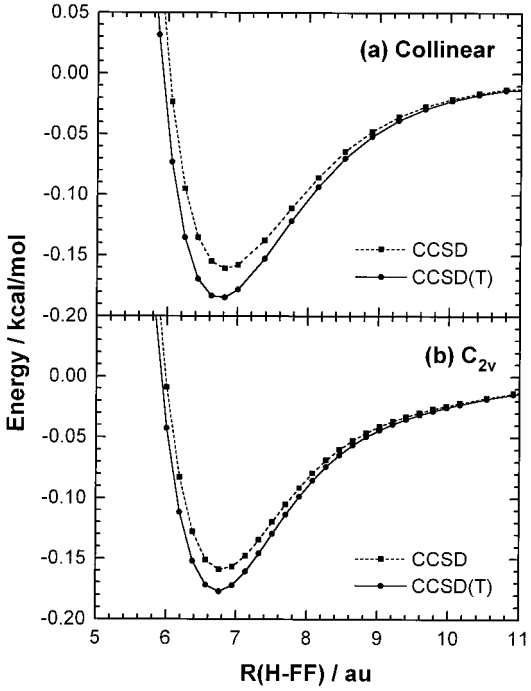

Figure 3. Long-range van der Waals potential calculated at the CCSD and CCSD(T) levels of theory as a function of the distance between the H atom and the midpoint of F_2 for (a) collinear and (b) C_{2v} geometries.

calculations should decrease so as to obtain a better agreement with the experimental activation energy because a larger bending frequency at the saddle point generally leads to a larger vibrationally adiabatic barrier height. This will be discussed later in detail.

Another important characteristic in which we are interested is a long-range van der Waals interaction in the asymptotic region of the potential surface. Although the van der Waals interaction is not generally taken into account in the potential energy surface, we expect that this may play an important role, especially in the reaction dynamics at low temperatures where quantum mechanical tunneling is dominant. Since the van der Waals interaction is an attractive force, this should result in a significant reduction of the barrier width for tunneling. Figure 3 shows the asymptotic potentials for H + F_2 calculated using the CCSD and CCSD(T) levels of theory. The internuclear distance of F_2 was set to be an equilibrium one. It can be seen that there exists a van der Waals well for both collinear and C_{2v} geometries. We find that the inclusion of triple excitation slightly increases the well depth. In addition, the well depth calculated at the CCSD(T) level of theory is found to be about 0.18 kcal/mol for both the collinear and C_{2v} geometries without zero-point energy correction. This indicates that the orientation of F_2 does not largely affect the depth of the van der Waals well. Schaefer and co-workers[1] also reported that the van der Waals wells exist in the asymptotic region of both the reactant and product channels. They found a small attraction, 0.05 kcal/mol, in the reactant H + F_2 channel and a stronger attraction, 0.55 kcal/mol, in the product HF + F channel. We did not calculate the van der Waals potential in the product channel since the van der Waals potential in the product channel is not be expected to largely affect the thermal rate constants for H + F_2. This is simply because the potential energy surface for the H + F_2 reaction has an "early barrier", and only characteristics of the potential energy surface in the entrance channel would be important for determining the thermal rate constants. However, such a van der Waals interaction in the product channel would presumably be important for calculating the product-state distributions.

3. Analytical Potential Energy Surfaces

Although the total number of energy values calculated by the ab initio method is large enough for carrying out a fitting to an analytical equation such as a many-body expansion form proposed by Sorbie and Murrell,[36] we employ a standard extended-LEPS function to develop a new potential energy surface. This is simply because the present ab initio MO calculations do not reproduce the experimental exothermicity, and the calculated classical barrier height may include an uncertainty of a few kcal/mol. Morse parameters employed are exactly the same as the JOT surface. However, two additional modifications were made to take into account the properties obtained from the ab initio calculations. The first one is that we use the angle-dependent Sato parameter[37,38] in the extended-LEPS function as follows:

$$\Delta_{HF} = \Delta^0{}_{HF} + a_{HF} \sin^2 \phi \qquad (1)$$

where ϕ is the angle defined by the intersection of the F−F internuclear axis and the vector connected from the H atom to the midpoint of the F−F bond. This modification was introduced to give a bending potential similar to the ab initio results. For F−F the Sato parameter Δ_{FF} is assumed to be constant. The second modification is that the following equation[39] was added to the extended-LEPS function so as to approximately reproduce the ab initio van der Waals potential in the asymptotic H + F_2 channel:

$$V_{vdW}(R) = -V_0 \exp[-\beta(R - R_0)^2] \qquad (2)$$

Here R denotes the distance between the H atom and the midpoint of F_2. V_0 and R_0 were set to be 0.22 kcal/mol and 7.4 a_0, respectively. β was set to be 0.18 for $R > R_0$, while 0.80 for $R < R_0$.

The parameters Δ_{FF}, $\Delta^0{}_{HF}$, and a_{HF} were determined so as that the saddle point geometry and bending potential approximately reproduce the ab initio results, except for the

TABLE 3: Sato Parameters Used in the Present LEPS Potential Surfaces

parameters	surface I	surface II
Δ_{HF}	−0.630	−0.613
Δ^0_{FF}	0.152	0.135
a_{HF}	−0.300	−0.300

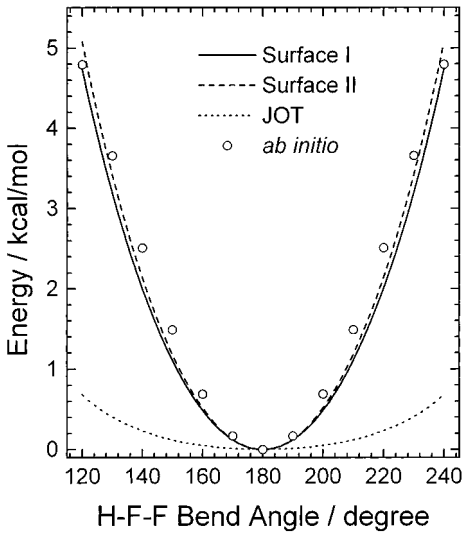

Figure 4. Comparison of H−F−F bend angle dependence of potential for various potential surfaces: surface I (solid line), surface II (dashed line), JOT surface (dotted line), and ab initio surface (open circle).

classical barrier height because the barrier height obtained from the present ab initio calculations is not reliable. Then, the thermal rate constants for the Mu(H) + F_2 reaction were calculated using reduced dimensionality theory,[33,34] which will be described in the following section, for a given set of parameters and compared to the experimental thermal rate constants for both the Mu + F_2 and H + F_2 reactions. Then, the root-mean-square of the differences between the calculated rate constants and the experimental rate constants were calculated. Extensive calculations have been done, and finally two potential surfaces giving the lowest two values of the root-mean-square have been selected. The only difference is the values used in the Sato parameters, which are summarized in Table 3. We denote these two surfaces as I and II. The saddle point properties of these new surfaces are summarized in Table 1. As can be seen, both surfaces I and II approximately reproduce the saddle point geometry obtained at the CCSD level of theory. The classical barrier heights for surfaces I and II are 0.7 and 1.0 kcal/mol, respectively, and are much smaller than the JOT value.

In Figure 4 we plot the bend angle dependence of potential energy at the saddle point. It can easily be seen that new potential surfaces reasonably well reproduce the ab initio results. On the other hand, the bending potential for the JOT surface is found to be unrealistic.

Table 4 presents the properties at the maximum of the vibrationally adiabatic potential[40,41] for both the H + F_2 and Mu + F_2 reactions. These properties were obtained from the vibrational analysis along the minimum-energy path. Note that the vibrational frequencies are slightly different from those in Table 1 because of the variational effect. The internuclear distance between H and F, R(H−F), for both surfaces I and II are smaller than that for the JOT surface; i.e., the JOT surface has a vibrationally adiabatic maximum that is earlier than surfaces I and II. It is interesting to note that the location of the vibrationally adiabatic maximum for the H + F_2 and Mu + F_2 reactions is quite similar for the JOT surface. On the other hand, for surfaces I and II, the location of the vibrationaly

TABLE 4: Properties at the Maximum of the Vibrationally Adiabatic Potential for the H + F_2 and Mu + F_2 Reactions

	JOT[a]	surface I	surface II
	H + F_2		
R(H−F)/Å	1.86	1.72	1.71
R(F−F)/Å	1.44	1.44	1.44
ΔV^{AG}/kcal/mol[b]	2.34	1.16	1.46
ω_{str}/cm^{-1}	774	782	774
ω_{bend}/cm^{-1}	63	212	218
	Mu + F_2		
R(Mu−F)/Å	1.83	1.52	1.55
R(F−F)/Å	1.44	1.44	1.44
ΔV^{AG}/kcal/mol[b]	2.73	2.66	2.91
ω_{str}/cm^{-1}	852	996	965
ω_{bend}/cm^{-1}	173	754	737

[a] Reference 31. [b] ΔV^{AG} is zero-point-inclusive barrier height relative to ground-state reactant; this quantity is called ΔV^{AG} in ref 41.

adiabatic maximum for Mu + F_2 is much later than that for H + F_2, indicating that the variational effect for surfaces I and II is more significant than that for the JOT surface. Note that this difference is mostly attributed to the difference in the bend frequencies, as can be seen in Table 4.

4. Reduced-Dimensionality Method

As mentioned earlier, we employed the reduced-dimensionality theory developed by Bowman[33,34] to calculate thermal rate constants for the H(Mu) + F_2 reaction because the theory is very easy to apply. The accuracy of the theory has extensively been studied for the H + H_2 and D + H_2 where accurate quantum results are available,[33,34,] although the accuracy of this theory is still unclear for the reaction with a large exothermicity. In the reduced-dimensionality theory of atom−diatom reactions, two stretch degrees of freedom are treated quantum mechanically, and the remaining bending motion is treated as an adiabatic bend during collision. Thus, the problem we have to solve reduces to a usual two-dimensional collinear quantum scattering problem.

The reduced-dimensionality Schrödinger equation was numerically solved using a standard **R**-matrix propagation on a natural collision coordinate system.[42] Bending vibrational energies were calculated on all the two-dimensional grid points using a standard harmonic basis set expansion method. The details of the computational procedure are described elsewhere.[33,34,43]

The scattering calculations were carried out only for the ground bending state. Therefore, the contribution of excited bending states to the rate constant was taken into account using a standard energy shifting approximation.[33,34] Thermal rate constants, $k(T)$, were thus calculated using the following equation:[33,34]

$$k(T) = \frac{Q^{\ddagger}_{rot}(T)\, Q^{\ddagger}_{bend}(T)}{hQ_{react}(T)} \int_0^{\infty} N(E) e^{-E/k_B T} dE \qquad (3)$$

where $Q^{\ddagger}_{rot}(T)$ and $Q^{\ddagger}_{bend}(T)$ are the rotational and bending partition functions at the variational transition state, respectively. These partition functions were calculated at the maximum of the vibrationally adiabatic potential (see Table 4). $Q_{react}(T)$ is the reactant partition function, which is the product of the internal partition function of F_2 and the relative translational partition function. h and k_B are Planck's constant and Boltzmann's constant, respectively. $N(E)$ is the reduced dimensionality cumulative reaction probability obtained from the scattering calculation and is given by the sum over all open initial and final vibrational states at the total energy E. Note that all of the tunneling correction are contained in $N(E)$.

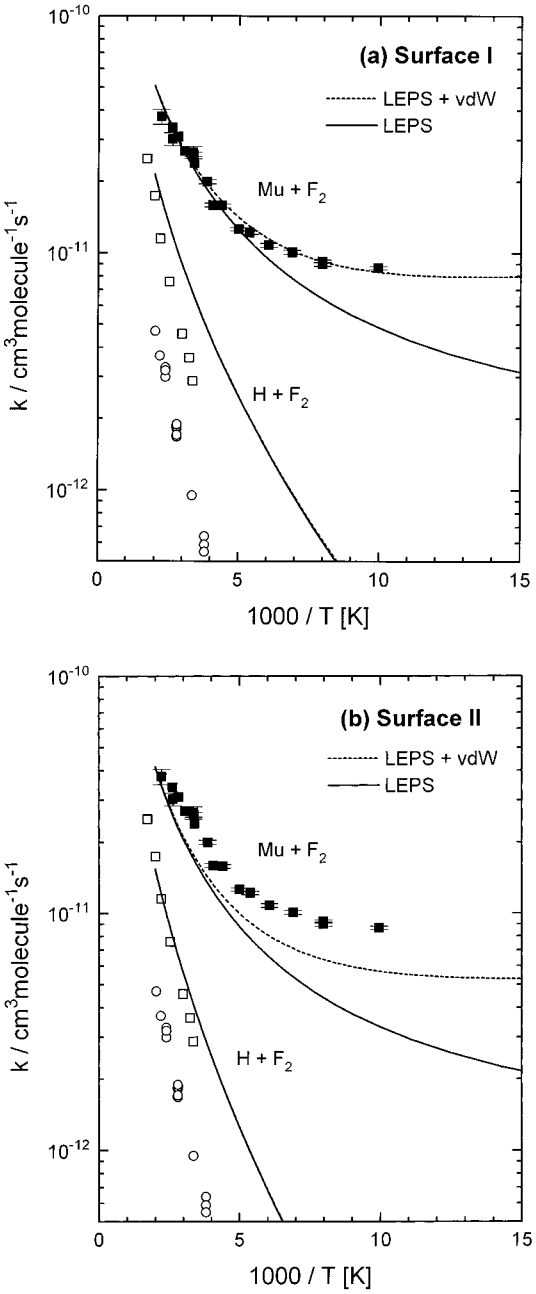

Figure 5. Arrhenius plot of rate constants calculated using (a) surface I and (b) surface II. Solid and dotted lines are the results calculated using the potential surface with and without van der Waals potential, respectively. Also shown are the Mu atom experimental data of Gonzalez et al. (closed square), the H atom data of Albright et al. (open square), and the H atom data of Homann et al. (open circle).

5. Thermal Rate Constants

First, we have to consider the effect of van der Waals potential on the rate constants. In Figure 5, we examine how the inclusion of a van der Waals potential affects the rate constants for both surfaces I and II. Solid lines in Figure 5 indicate the rate constants calculated using the potential energy surfaces without the van der Waals potential, while dotted lines show those calculated using the potential surface including the van der Waals potential given by eq 2. It can easily be seen that for the Mu + F_2 reaction the inclusion of the van der Waals potential significantly increases the rate constants, especially at low temperatures for both surfaces. For example, if we include the van der Waals potential in the potential energy surfaces, the rate constants become approximately double at about 100 K. In addition, it is noted that the rate constants

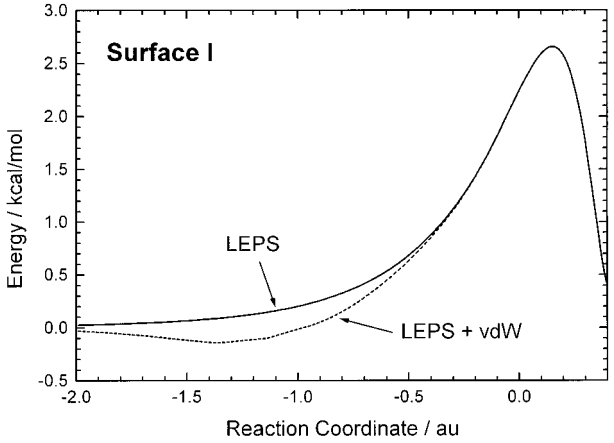

Figure 6. Vibrationally adiabatic potential curves along the minimum-energy path for surface I for the Mu + F_2 reaction. Solid line is calculated from the potential surface without van der Waals potential (LEPS), while dotted line is from the potential surface with van der Waals potential (LEPS + vdW).

calculated using the potential with the van der Waals interaction are approximately constant below 100 K, while the rate constants calculated using the potential surface without van der Waals interaction still decrease with a decrease in temperature. These results can be qualitatively understood in terms of the vibrationally adiabatic potential profile for the Mu + F_2 reaction plotted in Figure 6. As shown in Figure 6, since the LEPS potential is purely repulsive in the asymptotic region, the tunneling barrier width increases with a decrease in the translational energy. On the other hand, if we include the van der Waals interaction in the potential surface, the tunneling barrier width becomes a finite value with a decrease in the translational energy. These results imply that the barrier width is much more important than the barrier height at low temperatures where quantum tunneling is dominant. Figure 5 shows the contribution of the van der Waals interaction is, however, very small for the H + F_2 reaction. We find that the inclusion of the van der Waals interaction does not significantly affect the rate constants even at low temperatures down to 100 K. It is also noted that the depth of the van der Waals well for the Mu + F_2 reaction in Figure 6 is slightly small because of the nonzero bending frequency in this region.

In the comparison of the theoretical rate constants to the experimental ones, in Figure 5, the Mu + F_2 rate constants measured by Gonzalez et al. are in excellent agreement with theory for surface I. However, surface I overestimates the H + F_2 rate constants measured by Albright et al. and particularly by Homann et al. For surface II, on the other hand, the Mu + F_2 rate constants calculated are slightly smaller than the experimental ones, while for the H + F_2 reaction the theoretical results are comparable to the experimental results of Albright et al. Note that there exists considerable disagreement between the experimental results of Albright et al. and of Homann et al. for the H + F_2 reaction. This indicates that a further experimental study would be necessary to make quantitative comparison for H + F_2. Table 5 summarizes the reduced dimensionality rate constants calculated using surfaces I and II and compares them to the experimental results. As mentioned above, the rate constants calculated using surface II are slightly smaller than the experimental values at low temperatures; however, the difference in absolute value is only 35%. Thus, the agreement with experiment is quite satisfactory for both surfaces.

Table 6 shows the activation energies at 200 and 300 K obtained from the thermal rate constants for the Mu + F_2 and

TABLE 5: Comparison of Measured and Calculated Rate Constants (in cm^3 $molecule^{-1}$ s^{-1}) for the Mu + F_2 Reaction

T/K	exp[a]	surface I[b]	surface II[b]
101	8.7(−12)[c]	8.2(−12)	5.7(−12)
126	9.1(−12)	9.1(−12)	6.5(−12)
145	1.0(−11)	1.0(−11)	7.1(−12)
165	1.1(−11)	1.1(−11)	8.0(−12)
186	1.2(−11)	1.4(−11)	9.1(−12)
200	1.3(−11)	1.4(−11)	1.0(−11)
228	1.6(−11)	1.7(−11)	1.2(−11)
246	1.6(−11)	1.8(−11)	1.3(−11)
259	2.0(−11)	2.0(−11)	1.4(−11)
297	2.6(−11)	2.4(−11)	1.8(−11)
298	2.7(−11)	2.4(−11)	1.8(−11)
380	3.0(−11)	3.4(−11)	2.6(−11)
450	3.8(−11)	4.4(−11)	3.5(−11)

[a] Experimental results, ref 32. [b] Present work. [c] Numbers in parentheses indicate powers of 10.

TABLE 6: Comparison of Experimental and Theoretical Activation Energies, E_a(Mu) and E_a(H) (in kcal/mol)

T, K	surface I	surface II	exp
		Mu + F_2	
200	0.46	0.50	0.16 ± 0.08[a]
300	0.85	0.94	0.75 ± 0.08[a]
		H + F_2	
200	1.08	1.29	
300	1.41	1.64	2.4 ± 0.2[b]
			2.2 ± 0.1[c]

[a] Reference 32. [b] Reference 2. [c] Reference 3.

H + F_2 reactions. It can be seen that for the Mu + F_2 reaction the theoretical activation energies at 30 K for surfaces I and II are in good agreement with the experimental ones. For the H + F_2 reaction, on the other hand, the theoretical activation energies for both surfaces are found to be smaller than the experimental ones. It is also noted that the activation energies for Mu + F_2 are much smaller than those for H + F_2. This behavior has already been reported in earlier theoretical work,[16−22] where accurate quantum collinear calculations have been carried out on the JOT surface. Although the vibrationally adiabatic barrier height for Mu + F_2 is much larger than that for H + F_2 (see Table 4), the calculated activation energy for Mu + F_2 is smaller than that for H + F_2. This result clearly indicates that the quantum mechanical tunneling plays an essential role for Mu + F_2. One finds that for both surfaces I and II the activation energies for H + F_2 at 300 K are comparable to the vibrationally adiabatic barrier heights shown in Table 4. This implies that quantum mechanical tunneling is not so important for the H + F_2 reaction at 300 K. However, tunneling for this reaction should be important below 200 K since the activation energies at 200 K are smaller than those at 300 K.

Figure 7 plots the reduced dimensionality rate constants calculated using the JOT surface, which has been extensively employed in the previous dynamics calculations.[16−25,31] Also shown are the VTST rate constants[31] calculated by Garrett *et al*. Although Garrett et al. have not reported the VTST results below 200 K, the agreement with the present reduced dimensionality results is seen to be very good. Garrett et al. have calculated the contribution of quantum mechanical tunneling using the small-curvature semiclassical adiabatic ground-state (SCSAG) approximation.[31] The SCSAG method approximately accounts for the multidimensionality of the reaction in terms of the curvature of the reaction path. The good agreement between the VTST results and the present reduced-dimensionality results indicates that the reaction path method in the SCSAG approximation is quite realistic for both the Mu + F_2 and H + F_2 reactions. Although the reliability of the reduced-dimensionality method for the reaction with a large exothermicity is currently unclear, as mentioned in a previous section, the good agreement obtained in this work is encouraging.

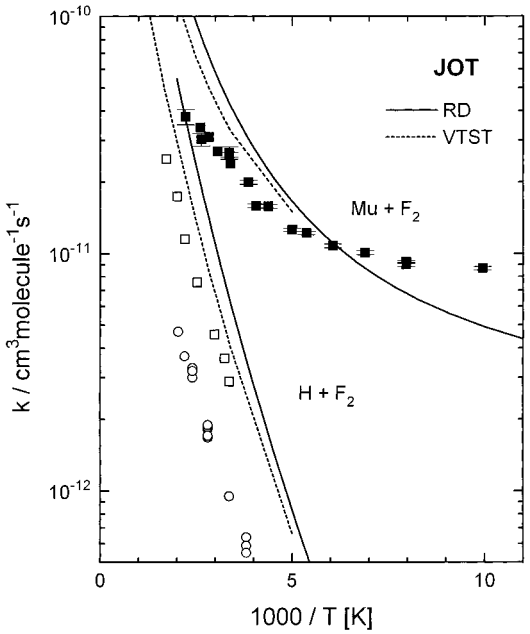

Figure 7. Arrhenius plot of reduced dimensionality rate constants calculated using the JOT surface (solid line). Dotted lines indicate the VTST results of Garrett et al. Closed and open squares and open circles indicate the experimental data (see Figure 5).

As Gonzalez et al. already noted,[32] the JOT rate constants for the Mu + F_2 reaction are larger at higher temperatures and smaller at lower temperatures than the experimental results. Comparison of Figures 5 and 7 quantitatively indicates that the rate constants calculated using the potential energy surfaces developed in this work give a better agreement than the JOT surface. Primary defects in the JOT surface are that the bending potential at the transition state is too shallow and that the surface does not include the van der Waals attractive interaction; a small bending frequency at the transition state would lead to too large a bending partition function at higher temperatures, while the ignorance of the long-range attractive interaction leads to an underestimate of quantum mechanical tunneling at lower temperatures.

The present work also suggests that the use of the LEPS type potential function would underestimate the contribution of quantum mechanical tunneling, especially at low temperatures since the LEPS potential is generally repulsive in the asymptotic region. In addition, tunneling correction using an Eckart potential[44] would not be a good approximation to predict a low-temperature behavior of the rate constants for the Mu + F_2 reaction since the Eckart potential is also repulsive and fails to account for the van der Waals mimima.

6. Summary

The potential energy surface for the H + F_2 reaction has been calculated by means of ab initio MO method at the CCSD/6-311++G(3DF,3PD) level of theory. Although the barrier height calculated at this level of theory is not yet reliable, important characteristics of the potential energy surface, including the location of the saddle point, the bend potential at the saddle point, and the long-range van der Waals potential, have been obtained. These data have been used to develop new potential energy surfaces. We have proposed two potential energy surfaces having the extended LEPS function form with slight

modifications. Thermal rate constants for the Mu + F_2 and H + F_2 reactions have been calculated by the reduced-dimensionality theory using the two new potential surfaces developed. Good agreements with experiment[32] have been obtained for the Mu + F_2 reaction within an error of 35% for both potential surfaces. However, a further experimental study would be needed to make a quantitative comparison for the H + F_2 reaction because of disagreement in the rate constants measured by two groups of researchers.[2,3]

It has been found that the van der Waals attractive force in the asymptotic region of the entrance channel of potential surface plays an essential role in determining the low-temperature behavior of the rate constants for the Mu + F_2 reaction. This is because the van der Waals potential reduces the width of the tunneling barrier significantly. The present work implies that otherwise the use of the LEPS type potential function would underestimate the contribution of quantum mechanical tunneling, especially at low temperatures, because the LEPS potential is generally repulsive in the asymptotic region. Although a further improvement of the potential energy surface for the H + F_2 reaction is necessary for more quantitative comparisons to experimental data, it should be emphasized that the conclusions derived from the present theoretical work are quite general in the field of chemical kinetics.

References and Notes

(1) O'Neil, S. V.; Pearson, P. K.; Shaefer III, H. F. *J. Chem. Phys.* **1973**, *58*, 1126.
(2) Albright, R. G.; Dodonov, A. F.; Lavrovsjaya, G. K.; Morosov, I. I.; Tal'rose, V. L. *J. Chem. Phys.* **1969**, *50*, 3632.
(3) Homann, R. H.; Schweinfurth, H.; Warnatz, J. *Ber. Bunsen-Ges. Phys. Chem.* **1977**, *81*, 724.
(4) Bender, C. F.; Bauschlicher, Jr., C. W.; Shaefer III, H. F. *J. Chem. Phys.* **1974**, *60*, 3707.
(5) Eades, R. A.; Dunning, Jr., T. H.; Dixon, D. A. *J. Chem. Phys.* **1981**, *75*, 2008.
(6) (a) Siegbahn, P.; Liu, B. *J. Chem. Phys.* **1978**, *68*, 2457. (b) Varandas, A. J. C.; Brown, F. B.; Mead, C. A.; Truhlar, D. G.; Blais, N. C. *J. Chem. Phys.* **1987**, *86*, 6258. (c) Boothroyed, A. I.; Keogh, W. J.; Matrin, P. G.; Peterson, M. R. *J. Chem. Phys.* **1991**, *95*, 4343. (d) Boothroyd, A. I.; Keogh, W. J.; Matrin, P. G.; Peterson, M. R. *J. Chem. Phys*. **1996**, *104*, 7139.
(7) Stark, K; Werner, H.-J. *J. Chem. Phys.* **1996**, *104*, 6515.
(8) Jonathan, N.; Okuda, S.; Timlin, D. *Mol. Phys.* **1972**, *24*, 1143.
(9) Polanyi, J. C.; Schreiber, J. L.; Sloan, J. J. *Chem. Phys.* **1975**, *9*, 403.
(10) Wilkins, R. L. *J. Chem. Phys.* **1973**, *58*, 2326.
(11) Pattengill, M. D.; Polanyi, J. C.; Schreiber, J. L. *J. Chem. Soc., Faraday Trans. 2* **1976**, *72*, 897.
(12) Jakubetz, W. *Chem. Phys.* **1978**, *35*, 129.
(13) Duggan, J. J.; Grice, R. *J. Chem. Phys.* **1983**, *78*, 3842.
(14) Firth, N. C.; Grice, R. *J. Chem. Soc., Faraday Trans. 2* **1987**, *83*, 1011.
(15) Last, I.; Baer, M. *J. Chem. Phys.* **1984**, *80*, 3246.
(16) Connor, J. N. L.; Jakubetz, W.; Manz, J. *Chem. Phys. Lett.* **1978**, *39*, 75.
(17) Connor, J. N. L.; Jakubetz, W.; Manz, J. *Chem. Phys.* **1978**, *28*, 219.
(18) Jakubetz, W. *Chem. Phys.* **1978**, *35*, 141.
(19) Connor, J. N. L.; Jakubetz, W.; Laganà, A. *J. Phys. Chem.* **1979**, *83*, 73.
(20) Connor, J. N. L.; Laganà, A. *Mol. Phys.* **1979**, *38*, 657.
(21) Connor, J. N. L.; Laganà, A.; Turfa, A. F.; Whitehead, J. C. *J. Chem. Phys.* **1981**, *75*, 3301.
(22) Jakubetz, W. *J. Am. Chem. Soc.* **1979**, *101*, 298.
(23) Clary, D. C.; Connor, J. N. L. *Chem. Phys. Lett.* **1979**, *66*, 493.
(24) Clary, D. C.; Connor, J. N. L. *J. Chem. Phys.* **1981**, *75*, 3329.
(25) Giménez, X.; Lucas, J. M.; Aguilar, A.; Laganà, A. *J. Phys. Chem.* **1993**, *97*, 8578.
(26) Ponalyi, J. C.; Sloan, J. J. *J. Chem. Phys.* **1972**, *57*, 4988.
(27) Jonathan, N.; Melliar-Smith, C. M.; Slater, D. H. *J. Chem. Phys.* **1970**, *53*, 4396.
(28) Sung, J. P.; Malins, R. J.; Setzer, D. W. *J. Phys. Chem.* **1979**, *83*, 1007.
(29) Dzelzkans, L. S.; Kaufman, F. *J. Chem. Phys.* **1982**, *77*, 3508.
(30) Tardy, D. C.; Feezel, L. L. *Chem. Phys.* **1988**, *119*, 89.
(31) (a) Garrett, B. C.; Steckler, R.; Truhlar, D. G. *Hyperfine Interact.* **1986**, *32*, 779. (b) Steckler, R.; Truhlar, D. G.; Garrett, B. C.; *Int. J. Quantum Chem. Symp*. **1986**, *20*, 495.
(32) Gonzalez, A. C.; Reid, I. D.; Garner, D. M.; Senba, M.; Fleming, D. G.; Arseneau, D. J.; Kempton, J. R. *J. Chem. Phys.* **1989**, *91*, 6164.
(33) Bowman, J. M. *J. Phys. Chem.* **1991**, *95*, 4960.
(34) Bowman, J. M.; Wagner, A. F. In *Theory of Chemical Reaction Dynamics*; Clary, D. C., Ed.; Reidel: Dordrecht, 1986; pp 47−76.
(35) Frisch, M. J.; Trucks, G. W.; Schlegel, H. B.; Gill, P. M. W.; Johnson, B. G.; Robb, M. A.; Cheeseman, J. R.; Keith, T.; Petersson, G. A.; Montgomery, J. A.; Raghavachari, K.; Al-Laham, M. A.; Zakrzewski, V. G.; Ortiz, J. V.; Foresman, J. B.; Cioslowski, J.; Stefanov, B. B.; Nanayakkara, A.; Challacombe, M. C.; Peng, Y.; Ayala, P. Y.; Chen, W.; Wong, M. W.; Andres, J. L.; Replogle, E. S.; Gomperts, R.; Martin, R. L.; Fox, D. J.; Binkley, J. S.; Defrees, D. J.; Baker, J.; Stewart, J. P.; Head-Gordon, M.; Gonzalez, C.; Pople, J. A. *Gaussian 94*; Gaussian, Inc.: Pittsburgh, PA, 1995.
(36) Sorbie, K. S.; Murrell, J. N. *Mol. Phys.* **1975**, *29*, 1387.
(37) Takayanagi, T.; Sato, S. *Chem. Phys. Lett.* **1988**, *144*, 191.
(38) Brown, F. B.; Steckler, R.; Schwenke, D. W.; Truhlar, D. G.; Barrett, B. C. *J. Chem. Phys.* **1985**, *82*, 188.
(39) Engel, V.; Schinke, R.; Pollak, E. *J. Chem. Phys.* **1987**, *87*, 1596.
(40) Garrett, B. C.; Truhlar, D. G. *J. Am. Chem. Soc.* **1979**, *101*, 4534.
(41) Garrett, B. C.; Truhlar, D. G.; Grev, R. S. In *Potential Energy Surface and Dynamics Calculations*; Truhlar, D. G., Ed.; Plenum: New York, 1980; pp 587−637.
(42) Light, J. C.; Walker, R. B. *J. Chem. Phys.* **1976**, *65*, 4272.
(43) Takayanagi, T.; Sato, S. *J. Chem. Phys.* **1990**, *92*, 2862.
(44) Eckart, C. *Phys. Rev.* **1930**, *35*, 1303.